SI: Cyclic dominance emerges from the evolution of two cooperative behaviors in the social amoeba

S. Shibasaki and M. Shimada

SI Text

Continuous replicator dynamics in the asexual model. First, we consider a model that ignores mating types and spatial structure. In this case, the payoff matrix A is given by [2] in the main text. This payoff matrix follows a rock-scissors-paper (RSP) game, if and only if

$$\begin{aligned} A_{21} > A_{11} > A_{31}, \\ A_{32} > A_{22} > A_{12}, \\ A_{13} > A_{33} > A_{23}, \end{aligned}$$

where A_{ij} is the element of matrix A in ith row and jth column. Using the inequalities $b_i > a_i \gg \epsilon_i > 0$ for $i = 1, 2$, we obtain

$$\begin{aligned} \frac{b_2 - a_2}{a_1 - \epsilon_0} &< \frac{1-\theta}{\theta}, \\ \frac{\epsilon_2}{h a_1 - \epsilon_0} &< \frac{1-\theta}{\theta}, \\ \frac{b_2 - a_2}{\epsilon_1 - \epsilon_0} &> \frac{1-\theta}{\theta}, \\ \frac{\epsilon_2}{h\epsilon_1 - \epsilon_0} &> \frac{1-\theta}{\theta}. \end{aligned}$$

It is reasonable to assume that $b_2 - a_2 \gg \epsilon_2$ due to the inequality $b_2 > a_2 \gg \epsilon_2 > 0$. If this inequality is satisfied, the condition for the RSP game is rewritten as

$$\frac{b_2 - a_2}{a_1 - \epsilon_1} < \frac{1-\theta}{\theta} < \frac{\epsilon_2}{h\epsilon_1 - \epsilon_0}.$$

The above left hand side can be simplified to $(b_2 - a_2)/a_1$ due to the inequality $a_1 \gg \epsilon_1$. If the new assumption $\epsilon_1 = \epsilon_2 \gg \epsilon_0$ is added, the right hand side is also simplified to h^{-1}. Note that this assumption is appropriate, because fruiting bodies and macrocysts would be more viable than vegetative cells under starvation, as they are dormant phases. From these approximations, the inequality in the main text [3] is derived.

Next, we show that the internal equilibrium G in the continuous replicator dynamics is a global attractor point if payoff matrix A (given by [2]) represents an RSP game. First, the payoff matrix A is transformed to $\tilde{A}$ by subtracting the diagonal elements from each column element:

$$\tilde{A}_{ij} \equiv A_{ij} - A_{jj}.$$

The transformed matrix $\tilde{A}$ also represents the RSP game if A does, and they have the same interior equilibrium. When the payoff matrix $\tilde{A}$ represents an RSP game, the interior equilibrium G is a unique global attractor (1, 2) if and only if

$$\det \tilde{A} = \tilde{A}_{21}\tilde{A}_{32}\tilde{A}_{13} + \tilde{A}_{31}\tilde{A}_{12}\tilde{A}_{23} > 0.$$

Notice that the diagonal elements of payoff matrix $\tilde{A}$ are 0s. The first and second terms are written, respectively, as

$$\begin{aligned} \tilde{A}_{21}\tilde{A}_{32}\tilde{A}_{13} &= (1-\theta)(b_1 - a_1)\left[(1-\theta)\theta h a_1 (b_2 - a_2) - \mathcal{O}(\max\{\epsilon_1, \epsilon_2\})\right], \\ \tilde{A}_{31}\tilde{A}_{12}\tilde{A}_{23} &= -\mathcal{O}(\epsilon_1^2). \end{aligned}$$

As ϵ_1 and ϵ_2 are very small, the second term is almost 0 while the first term is positive and larger than the absolute value of the second term. Here, we obtain $\det \tilde{A} > 0$.

Note that the condition wherein the interior equilibrium G is a global attractor in the discrete replicator dynamics is narrower than that in the continuous replicator dynamics. Fig. S1 shows both the conditions in the discrete replicator dynamics and an example of the evolutionary dynamics.

Cyclic dominance in the sexual model without spatial structure. When mating types are introduced, the payoff matrix is given by [6] in the main text. Here, we derive cyclic dominance, which is shown in Fig. 3 in the main text.

Note that only fruiting body formation occurs within the mating types, and therefore, defectors of fruiting body formation D^Fs beat the other two strategies within each mating type. In other words, D^Fs are unconditionally dominant over the other two strategies with the same mating types. In addition, the cooperators Cs beat the same mating type defectors of macrocyst formation D^Fs because these defectors cannot participate in fruiting body formation. For these reasons, we perform a pairwise analysis where the two strains have different mating types.

First, we analyze the case where the defectors of fruiting body formation D_i^F invade the other mating type defectors of macrocystsD_j^M $(i \neq j)$. The fitness of each strategy is given by

$$\begin{aligned} f\left(D_i^F\right) &= (1-\mu)\epsilon_1 + \mu(1-\theta)h\epsilon_1, \\ f\left(D_j^M\right) &= (1-\mu)\left\{(1-\theta)\epsilon_0 + \theta^* b_2\right\} + \mu\epsilon_0, \end{aligned}$$

where μ is the frequency of D_j^M. The difference in fitness between the two strategies is

$$f\left(D_j^M\right) - f\left(D_i^F\right) = \mu\left\{\epsilon_0 - (1-\theta)h\epsilon_1\right\} + (1-\mu)\left\{(1-\theta)\epsilon_0 + \theta b_2 - \epsilon_1\right\}.$$

It should be noticed that ϵ_i $(i = 0, 1, 2)$ is quite small. In $\epsilon_i \to 0$ limit, the difference in fitness is

$$f\left(D_j^M\right) - f\left(D_i^F\right) \to (1-\mu)\theta b_2 > 0.$$

Therefore, defectors of macrocyst formation D^Ms are unconditionally dominant over the other mating type defectors of fruiting body formation D^Fs.

The same analysis can be performed under different situations. The cooperator C_i $(i = 1, 2)$ is conditionally dominant over the other mating type defectors of fruiting body formation D_j^F or macrocyst formation D_j^M $(i \neq j)$. At the $\epsilon_i \to 0$ $(i = 0, 1, 2)$ limits, the conditions where C_i can beat the other mating types D_j^F and D_j^M are written, respectively, as follows:

$$\begin{aligned} a_1 &> (1-\theta)a_2 + \theta b_1, \\ a_1 &> (1-\theta)b_2. \end{aligned}$$

If these conditions are not satisfied, the strategies coexist at certain frequencies.

It should be noted that under the same strategies with different mating types (e.g., C_1 and C_2), neither strategy is dominant over the other. In these cases, it is necessary to compare the payoff from the interaction within mating types and the one expected between mating types. If the payoff from the interaction within mating types is larger, positive feedback selection works and the strategy with the larger initial frequency beats the other. If the expected payoff from the interaction between mating types is larger, negative frequency dependent selection works, and the two strategies coexist. Therefore, neither of the two strategies is dominant over the other, and this result holds across all pairs.

Experiment. It should be confirmed that fruiting body formation and macrocyst formation co-occur under some conditions. Previous research has shown that the FC cell fusion that occurs prior to macrocyst formation is prevented under light conditions (3) and that macrocyst formation is induced with excess water (4). By contrast, fruiting body formation is prohibited under water (5). Note that co-cultivation of the two different mating type strains of *D. discoideum* showed coexistence of fruiting bodies with the macrocysts under dark and dry conditions (6). It is unclear, however, whether conditions for this coexistence is sufficiently broad. We performed an experiment by co-cultivating the two mating types of *D. discoideum* under broader environmental conditions and estimated the range of conditions where fruiting bodies coexisted with macrocysts by using a support vector machine.

Materials and Methods. The methods and materials used in this experiment are almost the same as those in (6). Two heterothallic strains with different mating types of *D. discoideum*, Kax3 and V12, were used in the experiments. 20 spore balls were picked out from each strain and were suspended in 1 ml PB (20 mM KH_2PO_4, 20 mM $Na_2HPO_47H_2O$) supplemented with 2.7 mM $CaCl_2$ (namely PB*).

A fresh culture of *Escherichia coli* b/r was prepared as food in LB medium (per liter: 10 g Bacto tryptone [BD, Franklin Lakes, New Jersey, USA], 5 g yeast extract [BD], 10 g NaCl) with shaking (160 rpm for 2 h at 37 °C). The culture was centrifuged (15, 000 G for 30 s at 4 °C), and then, the supernatant was discarded and the same amount of PB was added. This procedure was repeated three times and the culture was suspended in PB*. The suspension of *E. coli* and *D. discoideum* was mixed at a rate of *E.coli* : Kax3 : V12= 3 : 1 : 1.

The mixed suspension was introduced in 6-well plates containing 3 ml of SM agar (per liter: 5 g glucose, 1.1 g KH_2PO_4, 0.9 g $Na_2HPO_47H_2O$, 5 g Bacto peptone [BD], 0.5 g yeast extract, agar 18 g). As previous research suggests that the amount of water can have an effect on the frequency of fruiting body formation and macrocyst formation (4, 5), different amounts of mixed suspensions were poured in each well (from 0.1 ml to 1.0 ml). To examine germination of both strains, either Kax3 or V12 was introduced into 2 of 6 wells on each plate (in these wells, the ratio of *E. coli* : Kax3 or V12 = 3 : 2).

The two strains of *D. discoideum* were co-cultivated under different light conditions at 22 °C for 7 days. The luminosity was measured before and after cultivation with an illuminometer (#78747, Shinwa, Niigata, Japan), and we used the means in the

analysis below. After cultivation, we examined whether both strains germinated, and we collected data from plates where the two strains germinated. First, the existence of fruiting bodies was examined with the naked eye. Then, each well was observed under an optical microscope to investigate whether macrocysts existed. Note that we ignored the numbers of fruiting bodies and macrocysts; the presence or absence was examined.

Data were classified into four categories: (i) only fruiting bodies exist, (ii) only macrocysts exist, (iii) both fruiting bodies and macrocysts exist, and (iv) neither fruiting bodies nor macrocysts exist. The raw data are shown in *SI_dataset*. The environmental conditions were normalized by z-scores. Then, the boundaries of the four categories were estimated by the linear support vector machine with Python using the function LinerSVC in the package scikit-learn (7). The parameter in LinerSVC, c was determined by 10-fold cross-validation. Note that we did not confirm that LinearSVC was the best model for classification, although the accuracy of the classification was about 0.85 (Fig. S7a).

Results. 206 data were collected and classified into 4 categories. 10-fold cross-validation suggested the value of parameter in LinearSVC $c = 5$ was the best value (Fig. S7a). The result of the classification is shown in Fig. S7b. As suggested in the previous study (6), fruiting bodies coexist with macrocysts under dark and dry conditions (lower left in S7b). In addition, both of them were formed with some amount of water (0.4 ml or 0.6 ml) under dark or low light conditions (about 300 lux). On the other hand, neither exists under light conditions with excess water (upper right). Dark conditions with excess water induced only macrocyst formation (upper left), whereas light conditions induced only fruiting body formation, unless in the presence of excess water (lower right). These results are consistent with those of previous research (3–6).

Evolutionary dynamics under the dynamic environment. In this section, we relax the assumption that fruiting bodies coexist with macrocysts by introducing dynamics into the environment. This model suggests the importance of the dynamical environment for the evolution of cooperative behaviors of fruiting body formation and macrocyst formation. Here, we used the model with mating types in the discrete replicator dynamics. We considered the two environmental factors: luminosity and amount of water around *D. discoideum*. We used the result of experiment shown in Fig. S7b to determine the class of the environment: (i) only fruiting bodies exist, (ii) only macrocysts exist, (iii) both fruiting bodies and macrocysts exist, and (iv) neither fruiting bodies nor macrocysts exist.

The environmental factors change the probability of macrocyst formation between the mating types θ according to the classes. As shown in Fig. S7b, fruiting bodies coexist with macrocysts under dark and relatively dry conditions, where we set the value of parameter as $\theta = 0.9$. Under light and dry conditions, only fruiting body formation occurs regardless of the mating types ($\theta = 0$); on the other hand, macrocyst formation always occurs between mating types ($\theta = 1$) and fruiting body formation never occurs under dark conditions with excess water, which means fruiting body formation does not provide any payoff under dark conditions with excess of water. Under light conditions with excess water, neither fruiting body formation nor macrocyst formation occurs and the frequencies of the strategies do not change.

We represent the two environmental factors z_1 (the luminosity) and z_2 (the amount of water). These values are normalized by z-score as we did in the analysis of the classification in the experiment. These two parameters are assumed to be updated as follows:

$$\mathbf{z}\left(t+1\right) \sim \mathcal{N}\left(\mathbf{z}(t), \Sigma\right)$$

where $\mathbf{z} = (z_1, z_2)$, and $\mathcal{N}\left(\boldsymbol{\mu}, \Sigma\right)$ is the multivariate normal distribution given the mean $\boldsymbol{\mu}$ and the covariance matrix Σ. In our model, therefore, the environmental condition at time $t+1$ is determined by the multivariate normal distribution whose mean is the environmental condition of the previous time step $\mathbf{z}\left(t\right)$ and covariance matrix is given by a constant matrix Σ:

$$\Sigma = \begin{pmatrix} \sigma^2 & 0 \\ 0 & \sigma^2 \end{pmatrix}.$$

The environmental condition of each time step is classified into four classes according to the result shown in Fig. S7b.

At the initial condition, the frequencies of all six strategies are equal while the initial environmental condition $\mathbf{z}(0)$ is given by the multivariate normal distribution whose mean is 0s and covariance matrix is

$$\begin{pmatrix} 1 & 0 \\ 0 & 1 \end{pmatrix}.$$

As shown in Fig. S8, the dynamics of the environment has a large effect on the evolutionary dynamics of cooperation both in fruiting body formation and macrocyst formation. If the environment where both fruiting bodies and macrocysts can be formed lasts, all six strategies coexist (Fig. S8a, b). However, the defectors of fruiting body formation or macrocyst formation are fixed when only fruiting body formation (Fig. S8c, d) or macrocyst formation (Fig. S8e, f) can be performed for a long time. These results show that our results in the main text do not always hold under the dynamic environment.

1. Nowak MA (2006) *Evolutionary dynamics exploring the equations of life.* (Belknap Press of Harvard University Press, Cambridge).
2. Broom M, Rychtar J (2013) *Game-Theoretical Models in Biology.* (Chapman and Hall/CRC), 1 edition, pp. 1–520.
3. Habata YY, Urushihara HH, Fang HH, Yanagisawa KK (1991) Possible existence of a light-inducible protein that inhibits sexual cell fusion in Dictyostelium discoideum. *Cell Struct. Funct.* 16(2):185–187.
4. Fang H, Sakuma T, Yanagisawa K (1992) Ammonia determines the alternative pathways of sexual or asexual development in the cellular slime mold Dictyostelium discoideum. *Devel. Growth Differ.* 34(4):373–378.
5. Bonner J (1947) Evidence for the formation of cell aggregates by chemotaxis in the development of the slime mold Dictyostelium discoideum. *The journal of experimental zoology* 106:1–26.
6. Shibasaki S, Shirokawa Y, Shimada M (2017) Cooperation Induces Other Cooperation: Fruiting Bodies Promote the Evolution of Macrocysts in Dictyostelium discoideum. *Journal of Theoretical Biology* 421:136–145.
7. Pedregosa F, et al. (2011) Scikit-learn: Machine learning in Python. *Journal of Machine Learning Research* 12:2825–2830.

SI figures

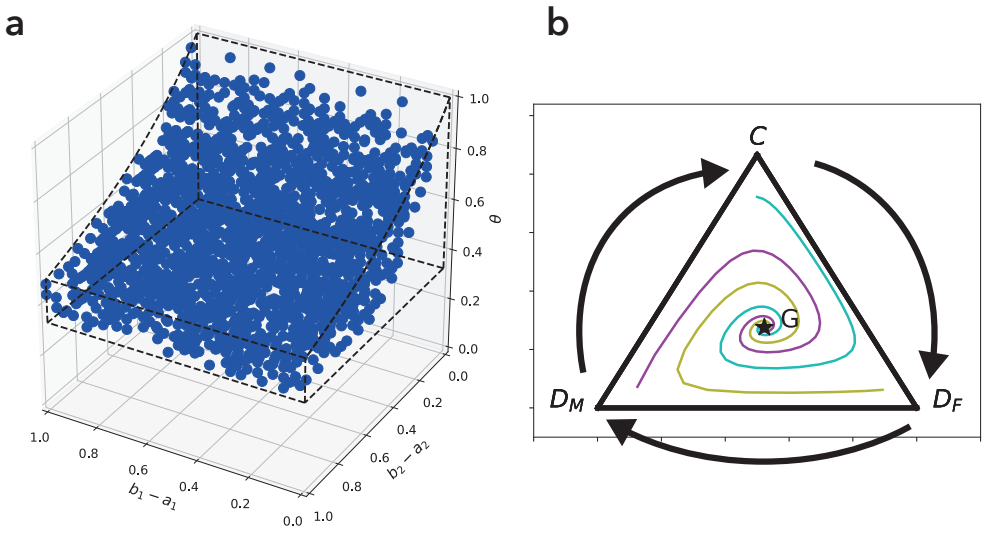

Fig. S1. Discrete replicator dynamics without mating types. In the discrete replicator dynamics, the interior equilibrium is not always stable if the payoff matrix represents the RSP game. The conditions where the interior equilibrium is stable in the discrete replicator dynamics are shown as blue dots, whereas those from the continuous replicator dynamics are inside the black dashed lines in (a). The parameters in (a) are $a_1 = 1$, $\epsilon_1 = 10^{-4}$, $a_2 = 0.5$, $\epsilon_2 = 10^{-4}$, $\theta = 0.5$, $h = 0.5$, and $\epsilon_0 = 10^{-6}$. The examples of the discrete replicator dynamics that converge to the interior equilibrium G are shown in (b). The parameters in (b) are $a_1 = 1$, $b_1 = 1.5$, $\epsilon_1 = 10^{-4}$, $a_2 = 0.5$, $b_2 = 1.2$, $\epsilon_2 = 10^{-4}$, $\theta = 0.5$, $h = 0.5$, and $\epsilon_0 = 10^{-6}$.

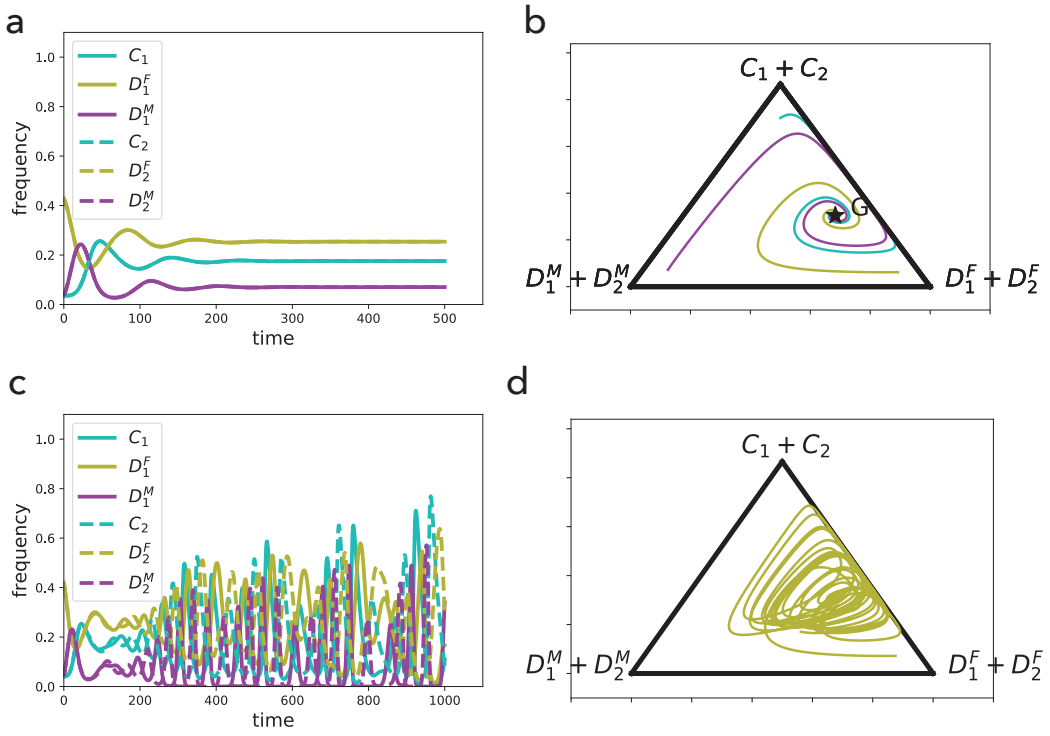

Fig. S2. Continuous replicator dynamics that include mating types. In these examples, there exists six strategies, and the initial sex ratio has a large effect on evolutionary dynamics. When the initial sex ratio is equal and the initial condition is symmetric over the mating types, the dynamics converge to the stable point (a), and this holds when the initial condition is changed (b). If the initial sex ratio is not equal (in this case $C_1 : D_1^F : D_1^M : C_2 : D_2^F : D_2^M = 1 : 10.1 : 1 : 1 : 10 : 1$), the dynamics never converge to the stable point (c).The dynamics in the phase space is shown in (d). Note that the cooperators C_1 and C_2 are not excluded even though the dynamics do not converge to the stable point. The parameters are $a_1 = 1$, $b_1 = 1.2$, $\epsilon = 10^{-4}$, $a_2 = 0.6$, $b_2 = 1.2$, $\epsilon_2 = 10^{-4}$, $\theta = 0.9$, $h = 0.5$, and $\epsilon_0 = 10^{-6}$.

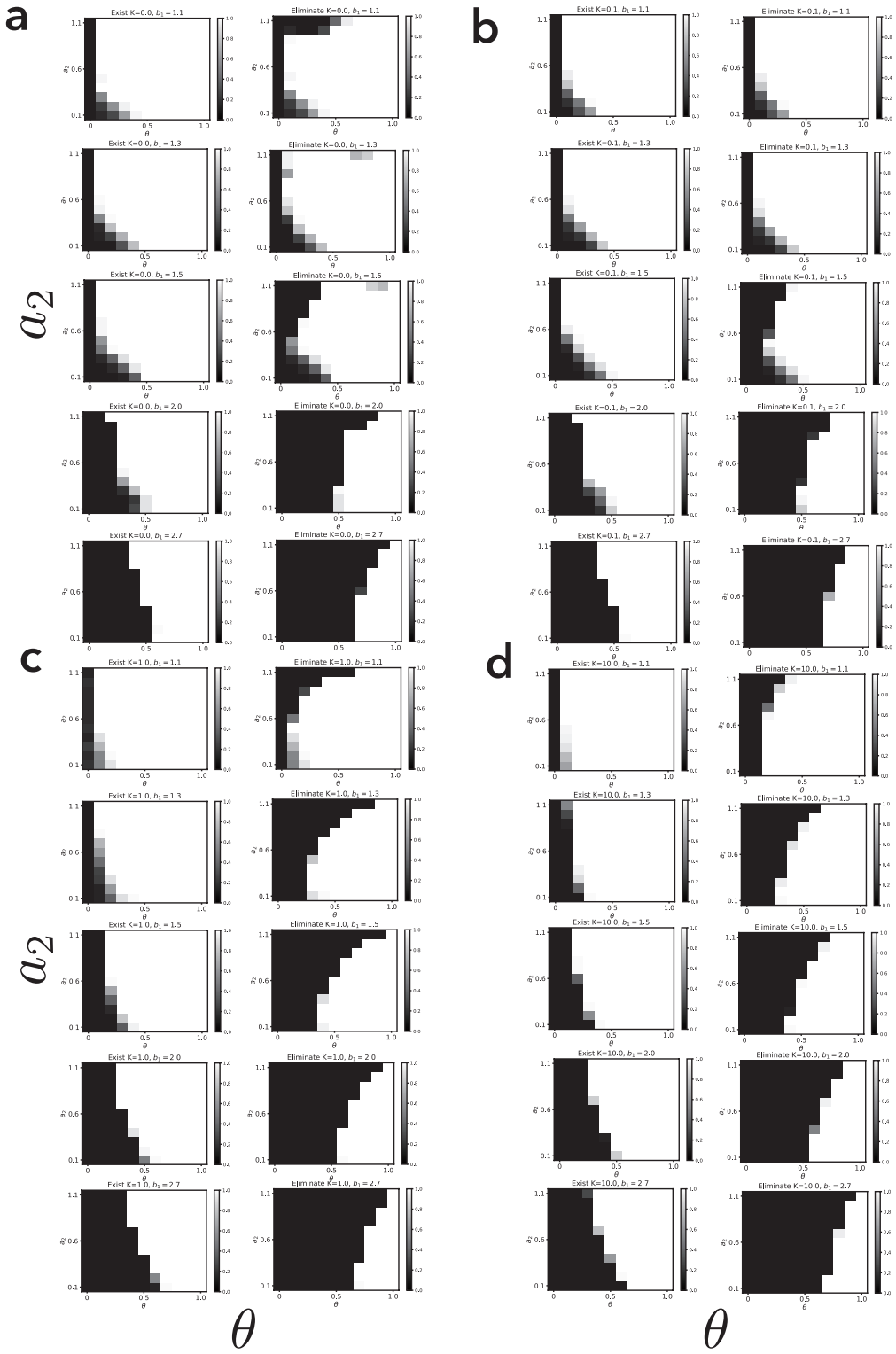

Fig. S3. Invasion of C_1 to D^F in the population in the agent-based model. We changed the strength of the selection (a: $K = 0$, b: $K = 0.1$, c: $K = 1$, and d: $K = 10$), benefit of exploitation in fruiting body formation ($b_1 = 1.1, 1.3, 1.5, 2.0, 2.7$), benefit of cooperation in macrocyst formation (a_2), and probability of macrocyst formation between mating types ($\theta = 0, 0.1, \ldots, 1.0$). Note that $\theta = 0$ represents the case when mating types of the two strategies are the same. The initial frequency of the invader is 0.01, and the frequency of the resident strategy is 0.99. If the frequencies of the invaders at the end of the simulation are more than 0.99, they can eliminate the resident strategies; if the invader's frequency is between 0.99 and 0.01, the invader can invade and coexist with the resident. Each box represents the probability of invasion success (left) or its elimination (right), given the parameter values. Regardless of the strength of selection, the cooperator C_1 cannot invade the same type of defector of fruiting body formation D_1^F, but it can invade and eliminate the counterpart of the other mating type D_2^F under some parameter values. The other parameters are $a_1 = 1$, and $\epsilon_1 = 10^{-5}$.

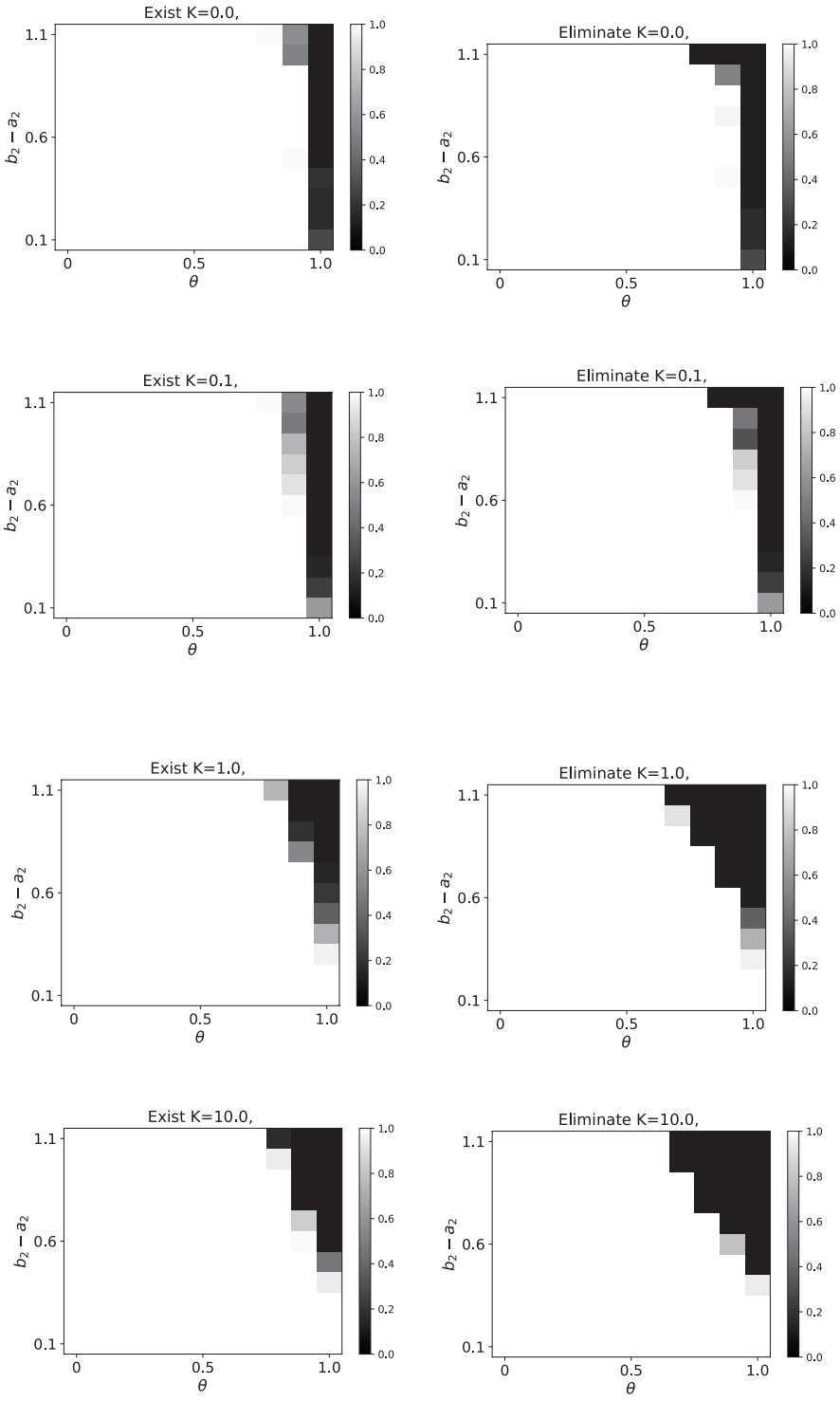

Fig. S4. Invasion of C_1 to D^M in the population in the agent-based model. Regardless of the strength of the selection, the cooperator C_1 can invade (left) and exclude (right) the same mating type defector of macrocyst formation D_1^M and the counterpart of the other mating type D_2^M unless θ is large. The other parameters are $a_1 = 1$, $a_2 = 0.5$, $\epsilon_2 = 10^{-5}$, $h = 0.5$, and $\epsilon_0 = 10^{-6}$.

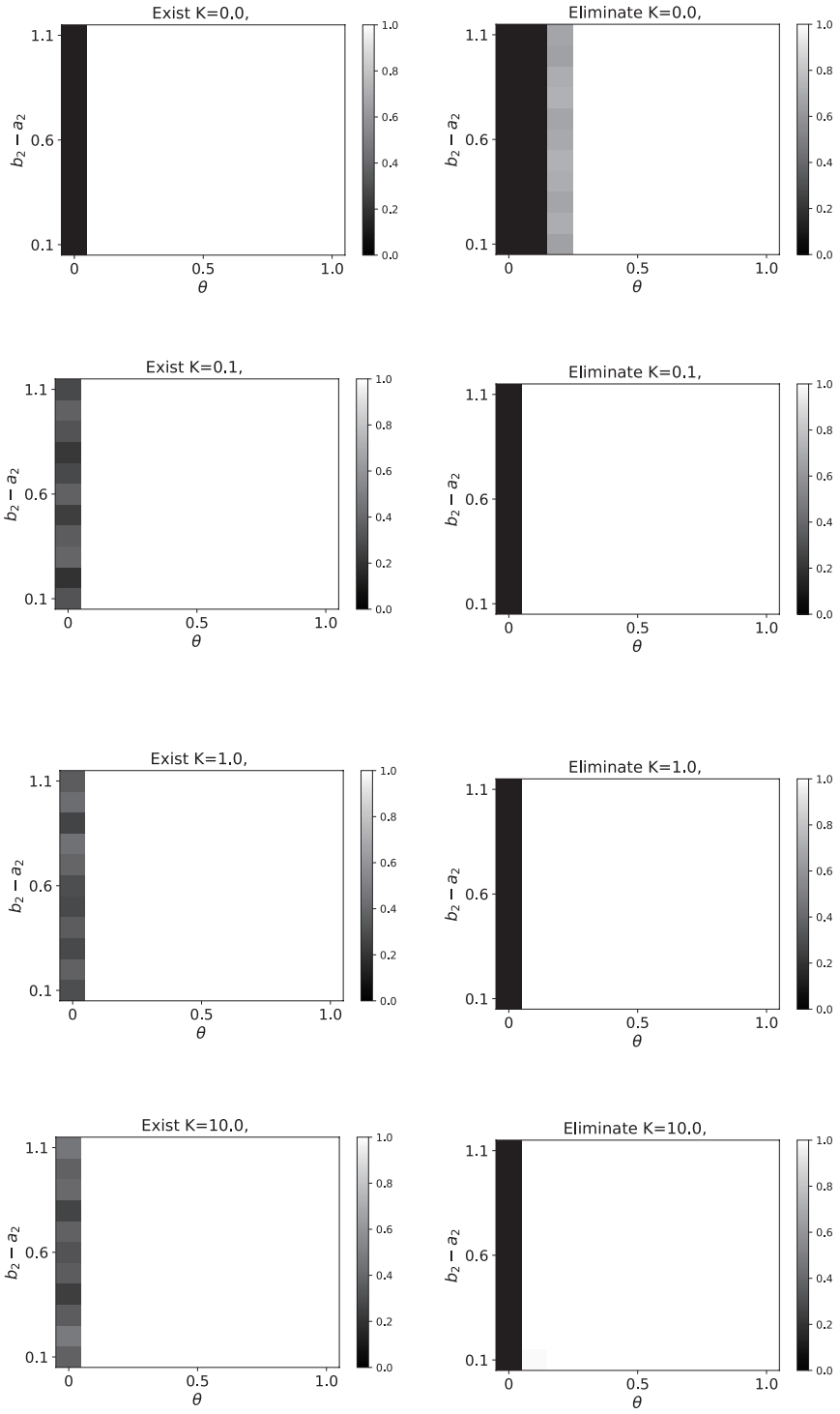

Fig. S5. Invasion of D_1^M to D^F in the population in the agent-based model. Regardless of the strength of the selection, D_1^M cannot invade the same mating type defector of fruiting body formation D_1^F, but it can invade the other mating type ones D_2^F. Unless selection is very strong ($K = 0.1, 1, 10$), D_1^M can exclude the other mating type defector of fruiting body formation. If $K = 0$, this exclusion occurs if $\theta \geq 0.3$. The other parameters are $\epsilon_1 = 10^{-5}$, $a_2 = 0.5$, $\epsilon_2 = 10^{-5}$, $h = 0.5$, and $\epsilon_0 = 10^{-6}$.

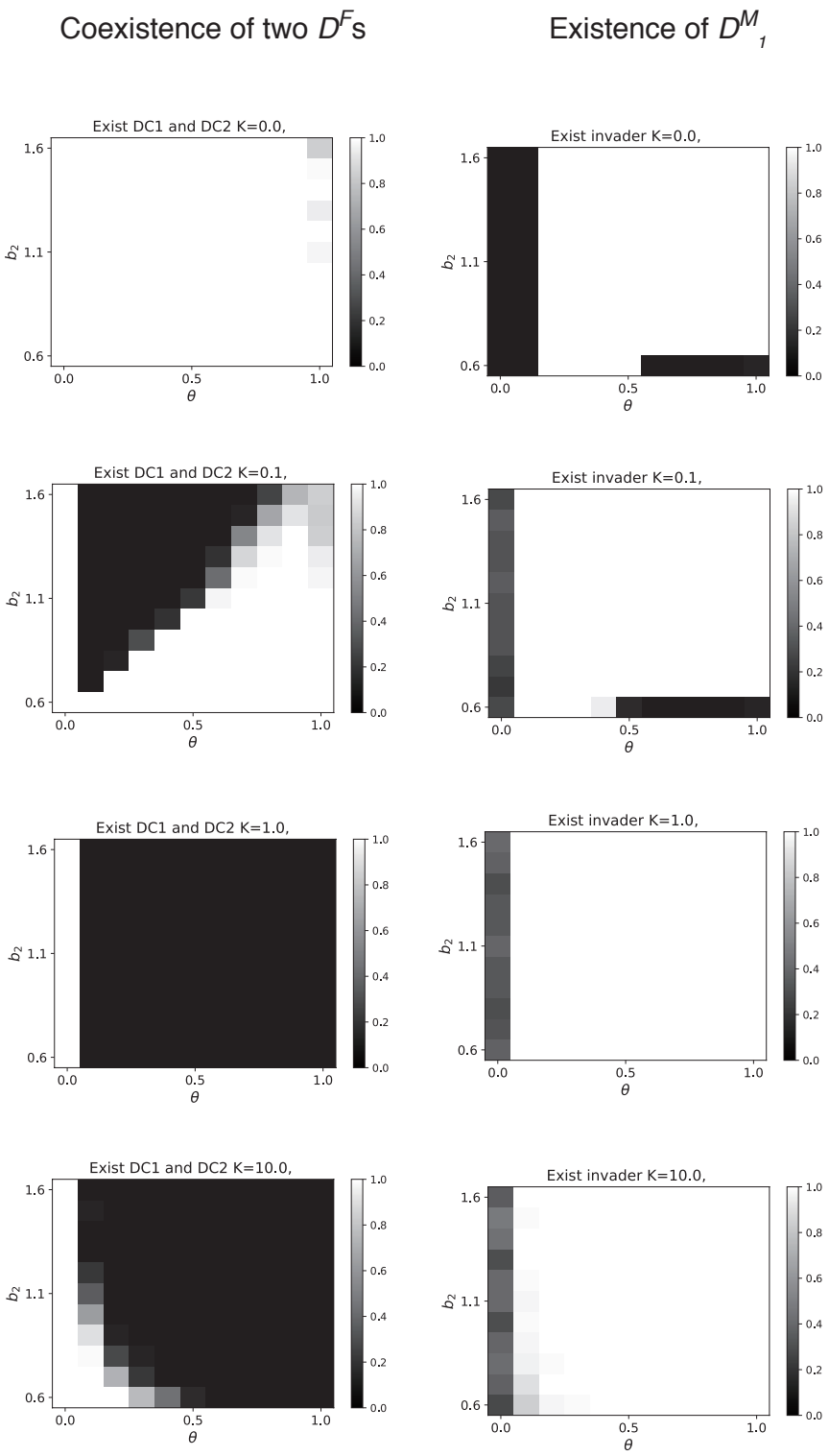

Fig. S6. Invasion of D_1^M into the population where D^Fs coexists in the agent-based model. The coexistence of D_1^F and D_2^F is an evolutionarily stable state if the defection of macrocyst formation does not occur. However, coexistence collapses due to the invasion of defectors of macrocyst formation D_1^M under weak selection ($K = 1, 10$, left column). On the other hand, the invader D_1^M can be maintained at a frequency greater than 0.01 regardless of the strength of selection under a wide range of parameter values b_2 and θ (right column). The other parameters are $\epsilon_1 = 10^{-5}$, $a_2 = 0.5$, $\epsilon_2 = 10^{[}-5]$, $h = 0.5$, and $\epsilon_0 = 10^{-6}$.

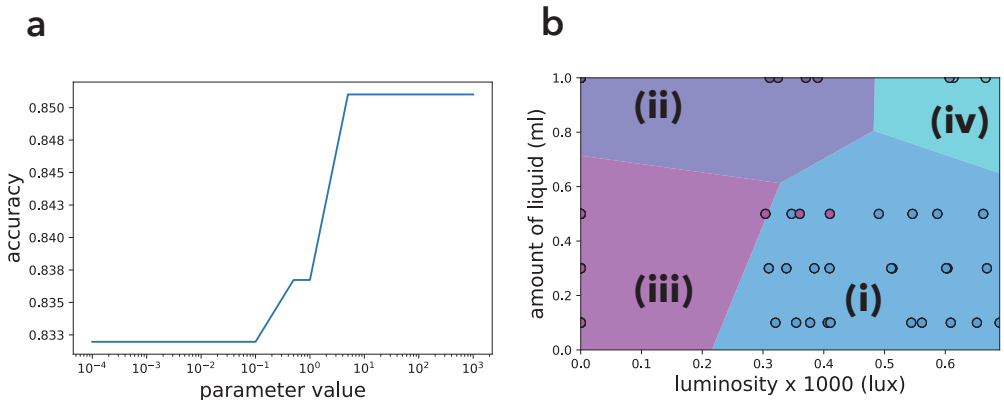

Fig. S7. Experimental results. The parameter for LinearSVC is adjusted by a 10-fold cross-validation (a). The result of classification is shown in (b). Under light and dry conditions (i), only fruiting bodies are formed, and only macrocysts are formed under dark conditions with a large amount of culture liquid (ii). Both fruiting bodies and macrocysts are formed under dark conditions with less liquid (iii), and neither is formed under light conditions with excess culture liquid (iv).

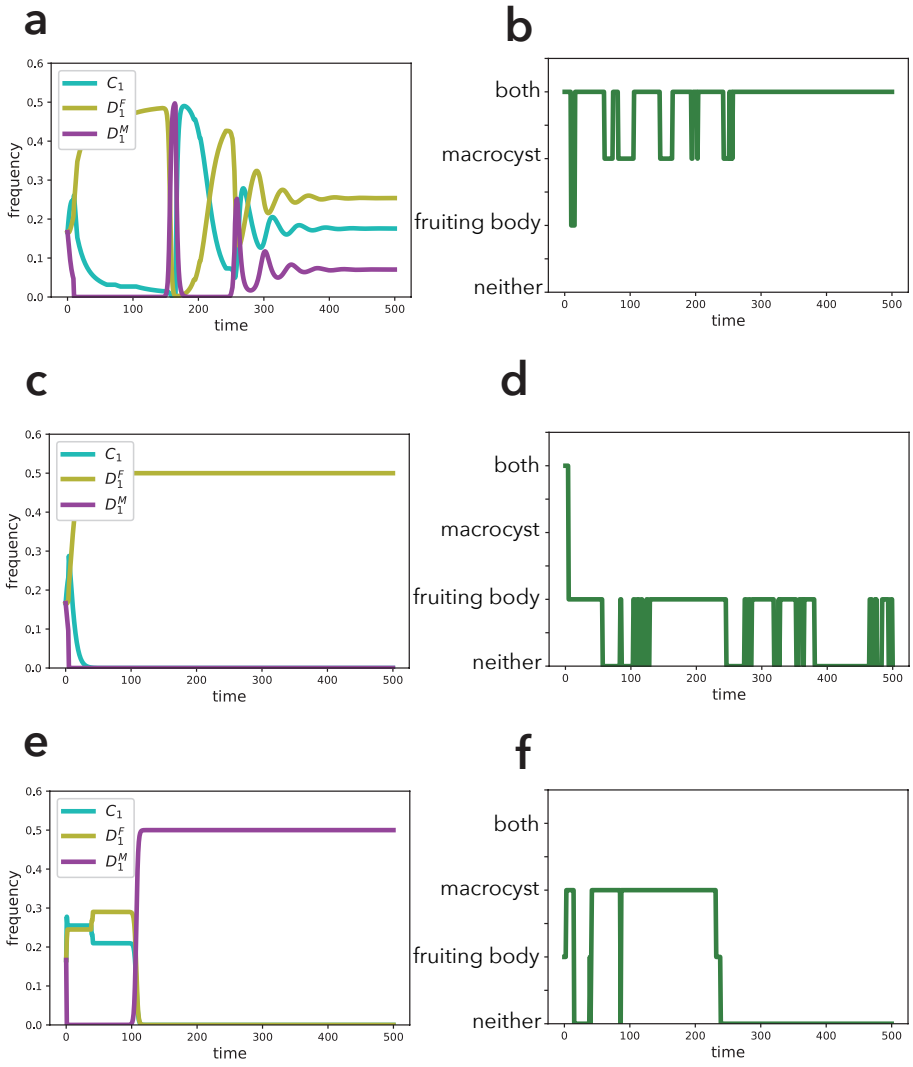

Fig. S8. Evolutionary dynamics under a dynamic environment. By introducing a changing environment, we relaxed the assumption that fruiting bodies coexist with macrocysts. In the initial condition, all six strategies coexist at the same frequencies. In the evolutionary dynamics, only the dynamics of mating type 1 are shown because the evolutionary dynamics are symmetric among mating types. Based on the environment, all strategies perform (i) only fruiting body formation, (ii) only macrocyst formation, (iii) both fruiting body formation and macrocyst formation, or (iv) neither fruiting body formation nor macrocyst formation. Three examples of the discrete replicator dynamics are shown in (a), (c), and (e) under environmental dynamics (b), (d), and (f), respectively. The environmental dynamics affect the results of the evolutionary dynamics. The parameters are $a_1 = 1, b_1 = 1.2, \epsilon_1 = 10^{-4}, a_2 = 0.6, b_2 = 1.2, \epsilon_2 = 10^{-4}, h = 0.5, \epsilon_0 = 10^{-6}$, and $\sigma = 0.05$. See SI text for the detail of the simulation.